A dissociative electron attachment cross-section estimator

2012 J. Phys.: Conf. Ser. 388 012013

(http://iopscience.iop.org/1742-6596/388/1/012013)

XXVII International Conference on Photonic, Electronic and Atomic Collisions (ICPEAC 2011) IOP Publishing
Journal of Physics: Conference Series **388** (2012) 012013 doi:10.1088/1742-6596/388/1/012013

A dissociative electron attachment cross-section estimator

James J. Munro,[1,2] Stephen Harrison,[1] Milton M Fujimoto[1,3] and Jonathan Tennyson[1]

[1] Department of Physics and Astronomy, University College London, Gower Street, London, WC1E 6BT, United Kingdom

.

[2] Quantemol Ltd., 37 Lancaster Grove, London, NW3 4HB, United Kingdom
[3] Universidade Federal do Paraná, Departamento de Física , 81531-990, Curitiba, Paraná, Brazil

E-mail: j.tennyson@ucl.ac.uk

Abstract. Dissociative electron attachment (DEA) is the major process where molecules are destroyed in low-energy plasmas. DEA cross sections are therefore important for a whole variety of applications but are both hard to measure or compute accurately. A method for estimating DEA cross sections based a simple resonance plus survival model is presented. Test results are presented for DEA of molecular oxygen and molecular chlorine, for which experimental measurements are available for comparison, and SiBr and $SiBr_2$, for which no previous data is available. The estimator has been implemented as part of Quantemol-N expert system which uses the R-matrix method to predict resonance positions and widths.

1. Introduction

Dissociative electron attachment (DEA) is the process whereby an incoming, low-energy electron attaches to a molecule causing it to fragment. Schematically this can be written as

$$AB + e^- \rightarrow A + B^- \quad \text{or} \quad A^- + B \tag{1}$$

where we have chosen to emphasise that DEA can often lead to a number of different products.

DEA is a key process in many low-energy plasmas [1]. For example in technological plasmas, which are widely used in plasma processing industry for a whole variety of reasons, DEA is usually the initial step which leads to the break-up for feedstock gases into radicals and ions. These, in turn, are the components which perform the plasma processing. A detailed knowledge of DEA is therefore important for understanding and modelling this processing procedure [2] and it has already been noted that theory can play an important role in providing the necessary information [3].

The basic process whereby most DEA occurs is initiated by an electron becoming temporarily trapped in a resonant state of the molecule. This resonance can either autoionize again, often leading to vibrational excitation of the target molecule, or, it can dissociate as in the manner of eq. (1). This second option occurs only if the energetics allow it and the resonance is long-enough lived for dissociation to occur. Theoretical models of DEA therefore require treatment of both

the electron and the nuclear dynamics [4]. Sophisticated theoretical treatments are available for DEA of a few key molecules such as hydrogen [5] and water [6]. However, in general, DEA processes have to be treated on a largely case-by-case basis and their study becomes significantly harder for larger molecules unless fairly drastic simplifications are made.[4]

In this paper we present a method for estimating DEA cross sections. The method is not designed to replace detailed calculations, or indeed high quality measurements, but rather to give a semi-quantitative estimate of the DEA cross section when no other, more reliable source of this information is available. The method is based on electron-molecule calculations performed with the R-matrix method [7] and is implemented as part of the Quantemol-N expert system [8]. Here we present results for DEA of oxygen and chlorine, molecules for which there are experimental data for comparison, and SiBr and $SiBr_2$, systems for which no previous studies are available.

2. Method

In our model the calculation is performed by computing two factors: a set of resonant cross-sections, which are the cross-sections (σ_r) for the electron colliding with the ground state target to form the resonance state and the survival probability (S) for the resonance, which is the probability of a molecule in that resonance state dissociating before is autoionizes. As a molecule may have several resonances, the total dissociative attachment cross-section is then given as a sum over the contribution from each of them:

$$\sigma_T(E) = C \sum_i S_i \sigma_{ri}(E) \tag{2}$$

where E is the incident electron energy, and i runs over the resonances being considered. The coefficient C is used to adjust the result to account for some of the physics missing from the model such as energy dependant widths for the resonances; in Quantemol-N this is set to 0.7.

The resonance cross-sections, σ_r, are computed from the resonance positions and widths. Whilst the survival probability uses a simple model for the target and resonance electronic potentials to predict a crossing point, the point at which the molecule must subsequently dissociate. Inputs for the calculation are a dissociation energy for the target, a ground state vibrational energy for the target and an electron affinity for the electron-attaching dissociating fragment, E_a. The only absolutely required input is dissociation energy for the target, D_e. A relatively arbitrary value of 1000 cm^{-1} is used for the vibrational energy, E_v, when it is not otherwise known. We have compiled an automatically accessed database of electron affinities for common fragments and this is used where possible.

The resonant cross-section is determined by the resonance position, E_r and width, Γ, which are determined automatically by fitting the computed eigenphase sums in the resonance region with a Breit-Wigner forming using program RESON [9]. The resonance cross sections calculated is a convolution of the Breit-Wigner cross-section over the vibrational ground state:

$$\sigma_r(E) = \int_0^\infty \Psi^*(r) \sigma_{BW}(E, r) \Psi(r) dr. \tag{3}$$

The wavefunction of the vibrational ground state is assumed to have a simple harmonic form

$$\Psi(r) = \left(\frac{2 m_r E_v}{\pi} \right)^{\frac{1}{4}} e^{-m_r E_v (r - R_e)^2}. \tag{4}$$

The Breit-Wigner cross-section is calculated using an adaptation of the standard formula

$$\sigma_{BW}(E, r) = \frac{2\pi}{E} \frac{\frac{1}{4}\Gamma^2}{(E - V_r(r))^2 + \frac{1}{4}\Gamma^2}. \tag{5}$$

where V_r is the resonance potential discussed below. While resonance energies and widths are taken directly from the R-Matrix calculation in Quantemol-N, the equilibrium distance for the molecule in the direction of the dissociating coordinate, R_e, is also needed. It is computed from the molecular geometry as the average distance of each atom from the centre-of-mass multiplied by a dimensional correction factor of $\sqrt{2}$.

A dissociation energy for the resonance state is computed simply as the difference between the target dissociation energy and the electron affinity of the dissociating fragment, $D_r = D_e - E_a$. A Morse potential is used to approximate the ground state electronic target potential in all cases with r as some notional dissociation coordinate. The target Morse potential is given by,

$$V_t(r) = (D_e - E_v)(1 - e^{\alpha(R_e - r)})^2 + E_v \tag{6}$$

where the width parameter α is obtained using

$$\alpha = \sqrt{\left(\frac{2\mu E_v^2}{D_e}\right)}. \tag{7}$$

R_e is the equilibrium distance for the target's ground state, and μ is the reduced mass of the target molecule. The reduced mass is estimated as the mass reduced between the dissociating electron-attached fragment and the remaining fragment

$$m_r = \frac{m_1 m_2}{m_1 + m_2} \tag{8}$$

where m_1 and m_2 are the masses of the two fragments.

The resonance potential can have two forms: it is assumed to be a decreasing exponential when the resonance energy is above the target dissociation energy and to be a Morse potential when the resonance energy is below the target dissociation energy (D_e). The Morse form is as given in eq. (2) and the exponential form is

$$V_r(r) = D_r + (E_r - D_r)e^{-2\alpha'(r - R_e)}, \tag{9}$$

where in both cases the resonance width parameter, α'. is taken to be $\alpha/2$; for the Morse curve this corresponds to assuming that the frequency of the vibrational fundamental for the resonance is half that of the neutral target.

The two potentials are then compared to find a crossing point r_c. If the anion reaches this point without autoionizing, then the molecule must dissociate. A survival probability (S) is then computed for this eventuality. When the crossing point r_c is less than the target equilibrium geometry r_e the survival probability is assumed to be unity ($S = 1$). When r_c occurs after r_e the survival probability is estimated by considering the classical time to reach r_c,

$$t = \sqrt{\frac{2m_e(r_c - r_e)^2}{V_r(r_e) - V_t(r_c)}} \tag{10}$$

and then the probability,

$$S = e^{-\Gamma t}. \tag{11}$$

3. Results

To calibrate the DEA estimator we have studied low-energy, electron-molecule collisions a number of molecules; here we present results for four molecules: Cl_2, O_2, SiBr and $SiBr_2$. All calculations used Quantemol-N [8] version 3.8 and only considered each molecule in its

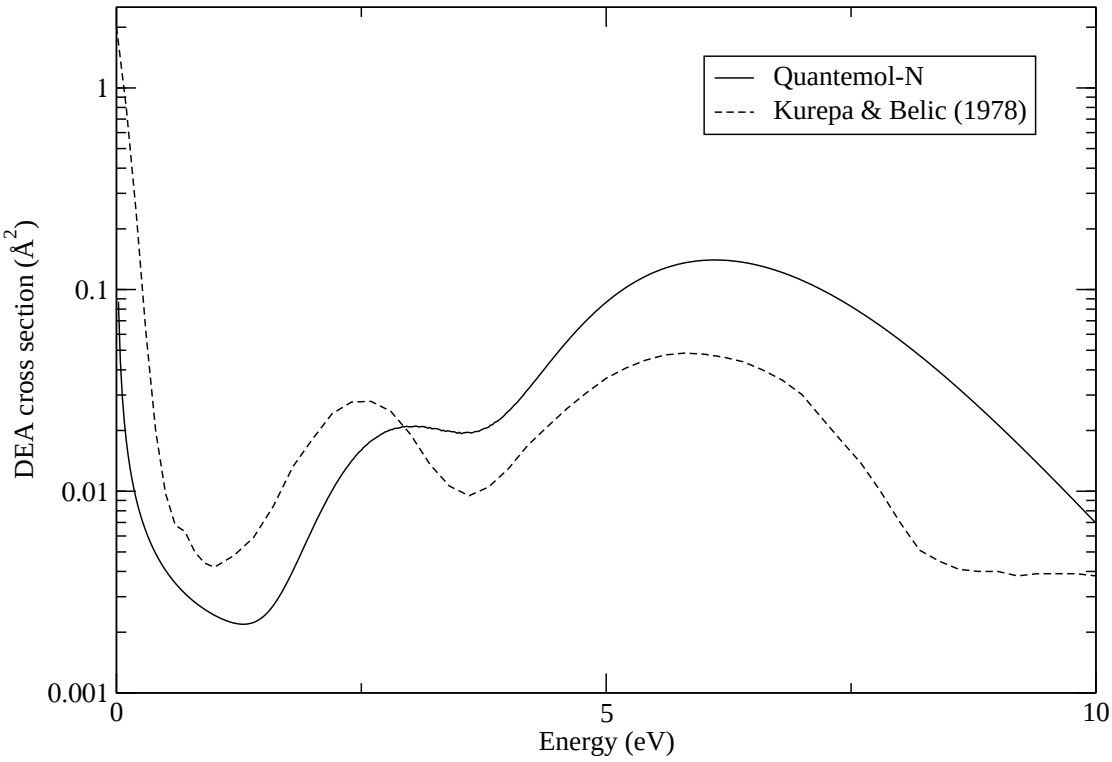

Figure 1. Dissociative electron attachment cross sections for Cl_2 as a function of electron impact energy as calculated using the DEA cross section estimator in Quantemol-N and as measured by Kurepa and Belic [13].

standard equilibrium geometry. Parameters not specified below used the default options chosen by Quantemol-N. Calculations were performed at the close-coupling level using a complete active space configuration interaction (CAS-CI) model for the target wavefunction and Hartree-Fock orbitals. All calculations used an R-matrix sphere of size 10 a_0 except for the one on $SiBr_2$ which used 13 a_0. A Gaussian type orbital (GTO) continuum basis sets appropriate to the R-matrix radius was taken from Faure *et al* [10].

The UK polyatomic R-matrix codes [11, 12] only uses Abelian point groups. This means that the calculation on Cl_2 and O_2 were performed using D_{2h} symmetry and those on SiBr and $SiBr_2$ used C_{2v} symmetry. In the case of $SiBr_2$, this the natural symmetry of the molecule in its equilibrium geometry. For the other molecules it is straightforward to re-cast the results into the true linear molecule symmetry which is therefore used below.

3.1. Chlorine

Calculations employed a DZP basis for the target for which a bondlength of 1.988 Å was used. A CAS-CI representation was employed in which 20 electrons are frozen in the ($1 - 3\sigma_g$, $1 - 3\sigma_u$, $1\pi_u$, $1\pi_g$) orbitals which correspond to the molecular orbitals formed from the Cl 1s, 2s and 2p orbitals. The 14 active electrons are distributed as: $(4 - 6\sigma_g, 4 - 5\sigma_u, 2\pi_u, 2\pi_g)^{14}$. The lowest virtual orbital of σ_g, σ_u and π_u were retained in the scattering calculation and the lowest 48 target states were retained in the close-coupling expansion.

To estimate dissociative attachment cross-section the following values were used: vibrational frequency, $E_v = 1000$ cm^{-1}; Cl_2 dissociation energy, $D_e = 2.48$ eV and chlorine atom electron

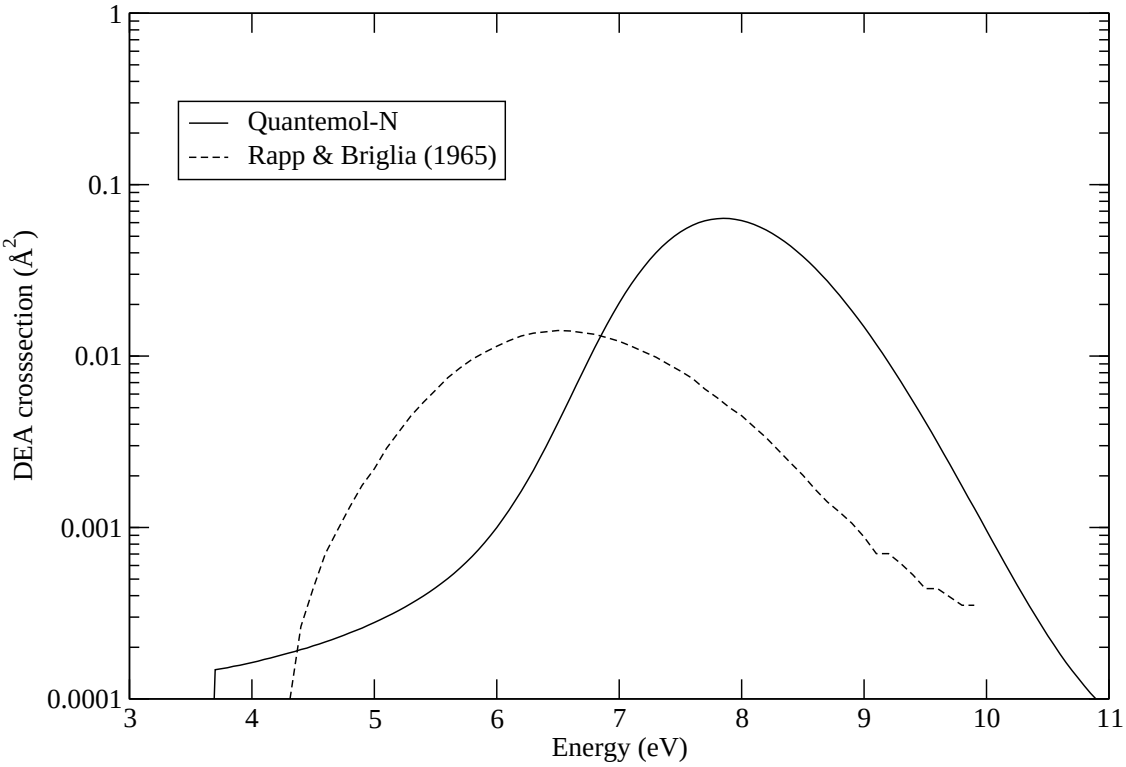

Figure 2. Dissociative electron attachment cross sections for O_2 as a function of electron impact energy as calculated using the DEA cross section estimator in Quantemol-N and as measured by Rapp and Briglia [16].

affinity $E_a = 3.62$ eV.

Electron collisions with Cl_2 give a complicated resonance structure and our Quantemol-N calculations finds a very narrow $^2\Pi_g$ at 3.2 eV with a width of 0.9 meV, a $^2\Pi_u$ at 6.4 eV with a width of 20 meV and a broader $^2\Sigma_g$ resonance at 7.2 eV with a with of 0.53 eV. These are all considered in our estimate of the DEA cross section.

DEA of Cl_2 has been studied experimentally by Kurepa and Belic [13] and using a semi-empirical R-matrix method by Fabrikant *et al* [14]. Tam and Wong [15] gave a considerably less comprehensive experimental study at the same time as Kurepa and Belic. Figure 1 compares our calculation with the measurements of Kurepa and Belic. Our estimates reproduce the structure of measured cross sections well with semi-quantitative agreement for the magnitudes.

4. Oxygen

Calculations used a 6-311G* basis for the target which was frozen at a bondlength of 1.2144 Å. The target CAS employed froze the 4 core electrons and distributed the remaining 10 electrons amongst 12 valence orbitals, this can be writen $(1\sigma_g, 1\sigma_u)^4$ $(2\sigma_g, 3\sigma_g, 2\sigma_u, 3\sigma_u, 1\pi_u, 2\pi_u, 1\pi_g)^{12}$. The scattering calculation was augmented with the $4\sigma_g$, $4\sigma_u$ and $2\pi_g$ orbitals. 48 states were retained in the outer region close-coupling calculation.

DEA estimates used a vibrational frequency of 1580 cm^{-1}, an O_2 dissociation energy of 5.116 eV and an O^- electron affinity of 1.461 eV. It is well known that O_2 supports a low-energy $^2\Pi_u$ resonance and a $^2\Pi_g$ resonance at about 7.5 eV [17, 18]. The former is too low in energy to

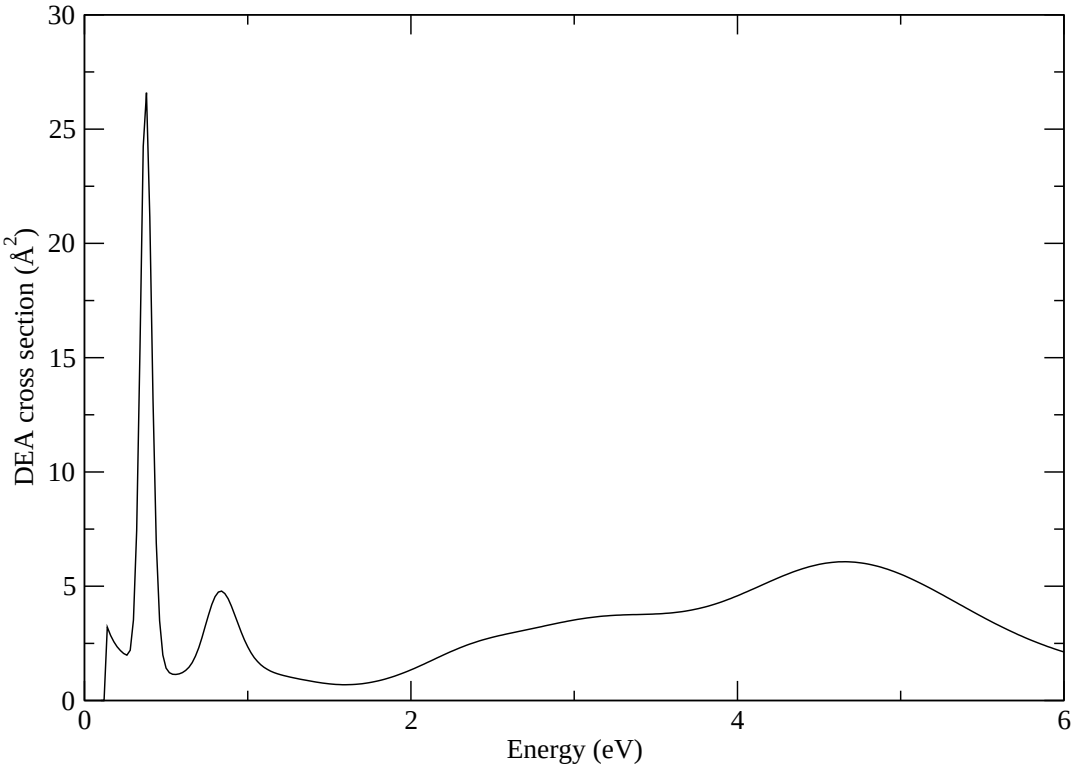

Figure 3. Estimated dissociative electron attachment cross sections for SiBr as a function of electron impact energy.

make a significant contribution to the dissociative attachment cross section. Our Quantemol-N calculations find the $^2\Pi_g$ resonance at 7.3 eV with a width of 0.45 eV. We did not consider the possible effect of the high-energy $^4\Sigma_u^+$ resonance [19].

Comparisons with the measurements of Rapp and Briglia [16], see Fig. 2, give reasonable agreement and suggest that the calculated resonance position is slightly too high.

5. SiBr

Our calculations used a 6-311G basis and a fixed SiBr bondlength of 2.64 Å. Our CAS-CI representation was $(1-8\sigma\ 1-3\pi)^{28}\ (9-13\sigma\ 4-6\pi\ 1\delta)^{21}$ which corresponds to freezing all the inner electrons and distributing the valence electrons freely amongst all valence orbitals. The scattering calculations were augmented by two extra σ and one extra π orbitals. It should be noted that our calculations suggest that SiBr has a relatively low ionisation potential of 4.5 eV.

The dissociative attachment cross-section estimator used a vibrational frequency of 1000 cm^{-1}, a dissociation energy of 3.5 eV and an electron affinity for Br of 3.36 eV. Our SiBr calculations displayed an unusually large number of resonances. There are several reasons for this: first SiBr is an open shell system which means there are low-lying unoccupied orbitals which are available for resonance formation; to these can be added a low-lying, empty d orbital on the Br which can also be occupied in resonance states. Second, SiBr has an odd number of electrons which means that the $N+1$ electron scattering system can form both singlet and triplet states. Many resonances appear with both spin symmetries. Finally, the low ionisation energy of SiBr leads to large numbers of resonances being detected in our calculations above

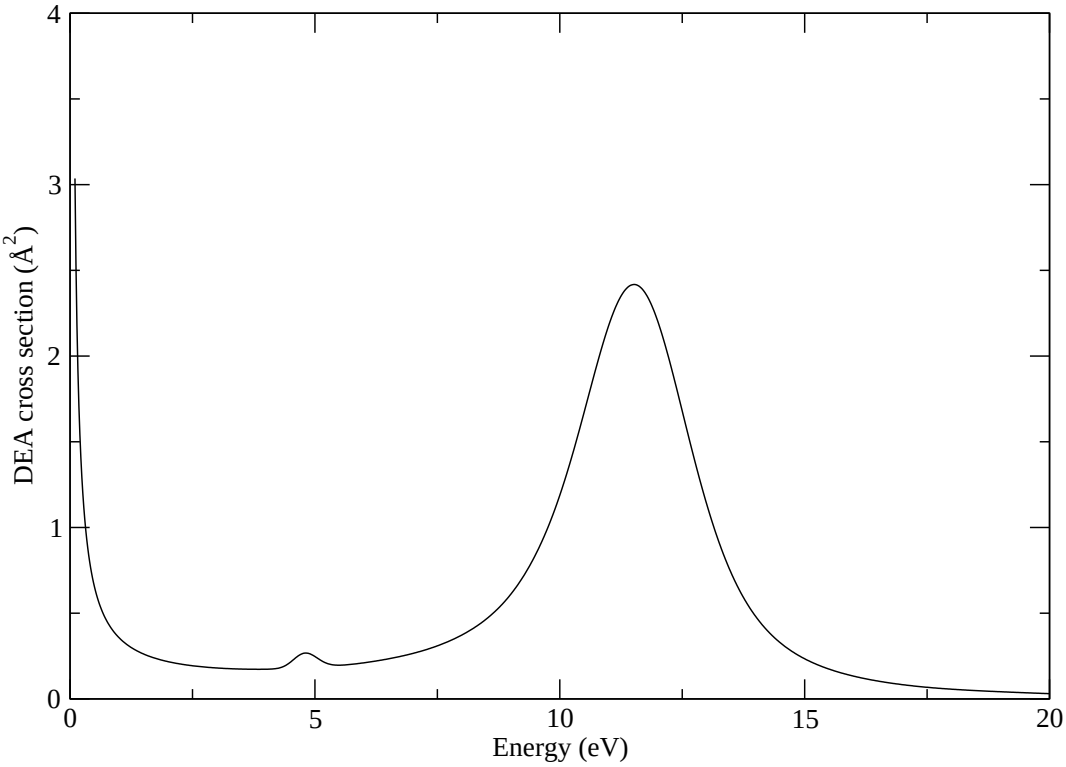

Figure 4. Estimated dissociative electron attachment cross sections for $SiBr_2$ as a function of electron impact energy.

5 eV. These so-called pseudo-resonances are an artifact of a calculation which does not allow for an ionisation channel [7]. For this reason we only consider the DEA cross section up to 5 eV; however we note that in practise our estimator procedure does not assign large cross sections to the pseudo-resonances.

Figure 3 shows our estimated DEA cross section; there are no previous studies on this process for us to compare with. Analysis of our calculations shows that the low-energy spike is due to narrow $^3\Pi$ and $^1\Pi$ resonances at 0.380 and 0.385 eV respectively, both with widths about 0.004 eV. The next feature can be associated with $^3\Sigma^+$ and $^1\Sigma^+$ resonances at 0.840 and 0.863 eV respectively and widths about 0.005 eV.

6. $SiBr_2$

Calculations were performed on $SiBr_2$ using a frozen geometry with the SiBr bondlengths set to 2.28 Å and bondangle of 103.1^o, and using a 6-311G basis set. 62 inner shell electrons were frozen with the remaining 22 valence electrons distributed amongst 13 valence orbitals. A further 3 "virtual" orbitals were retained in the scattering calculation. $SiBr_2$ is a closed shell system and our calculations suggest that its ionisation potential is close to 10 eV, substantially higher than SiBr.

DEA cross sections were estimated using a vibrational frequency of 118.7 cm^{-1} in the effective dissociation coordinate, an energy for dissociating a Br atom of 3.16 eV and a Br electron affinity of 3.36 eV. Note that the Br electron affinity is sufficient to mean that the DEA channel is open at all energies. Our calculations find a low-lying $^2A_1$ resonance at 0.24 eV with a width of 0.22 eV

does indeed provide a mechanism for DEA in the threshold region. $SiBr_2$ has significantly fewer resonances than SiBr but still shows other DEA peaks, see fig. 4, which are all due to the combined effects of several resonances.

7. Conclusion

We present a method for estimating dissociative electron attachment (DEA) cross sections which we have implemented as an option in the Quantemol-N expert system. The method is particularly useful for cases where there are no other data available for this process.

Comparisons with measured DEA cross sections for O_2 and Cl_2 show reasonable agreement. The most significant difference from the measurements is that the resonances are, in general, slightly too high in energy. This issue is not to do with our estimator but with the underlying R-matrix calculations. We note that these calculations are based on the use of relatively small basis sets and could undoubtedly be improved by a better treatment of polarisation such as that offered by the molecular R-matrix with pseudostates (RMPS) method [20, 21].

Our DEA estimator is applied to SiBr and $SiBr_2$, which are important products of the etching of silicon wafers by bromine atoms and ions. The DEA cross sections here have been used as part of an improved model of silicon etching [22] which explains that the observed improvement in etch properties with pressure was actually due to the increased presence of these species in the etching gas.

References

[1] Morgan W 2000 *Adv. At. Mol. Opt. Phys.* **43** 79 – 110
[2] Kimura M 2001 *Adv. At. Mol. Opt. Phys.* **44** 33 – 57
[3] Winstead C and Mckoy V 2000 *Adv. At. Mol. Opt. Phys.* **43** 111 – 145
[4] Fabrikant I I 2010 *J. Phys. Conf. Ser.* **204** 012004
[5] Celiberto R, Janev R K, Wadehra J M and Tennyson J 2012 *Chem. Phys.* **398** 206–213
[6] Haxton D J, Rescigno T N and McCurdy C W 2007 *Phys. Rev. A* **75** 012711
[7] Tennyson J 2010 *Phys. Rep.* **491** 29–76
[8] Tennyson J, Brown D B, Munro J J, Rozum I, Varambhia H N and Vinci N 2007 *J. Phys. Conf. Series* **86** 012001
[9] Tennyson J and Noble C J 1984 *Comput. Phys. Commun.* **33** 421–424
[10] Faure A, Gorfinkiel J D, Morgan L A and Tennyson J 2002 *Comput. Phys. Commun.* **144** 224–241
[11] Morgan L A, Tennyson J and Gillan C J 1998 *Comput. Phys. Commun.* **114** 120–128
[12] Carr J M, Galiatsatos P G, Gorfinkiel J D, Harvey A G, Lysaght M A, Madden D, Masin Z, Plummer M and Tennyson J 2012 *Euro. J. Phys. D* **66** 58
[13] Kurepa M V and Belic D S 1978 *J. Phys. B: At. Mol. Phys.* **11** 3719–3729
[14] Fabrikant I I, Leininger T and Gadea F X 2000 *J. Phys. B: At. Mol. Opt. Phys.* **33** 4575–4580
[15] Tam W C and Wong S F 1978 *J. Chern. Phys.* **68** 5626–5630
[16] Rapp D and Briglia D D 1965 *J. Chem. Phys.* **43** 1480–1489
[17] Noble C J and Burke P G 1992 *Phys. Rev. Lett.* **68** 2011–2014
[18] Tashiro M, Morokuma K and Tennyson J 2006 *Phys. Rev. A* **73** 052707
[19] Prabhudesai V S, Nandi D and Krishnakumar E 2006 *J. Phys. B: At. Mol. Phys.* **39** L277–L283
[20] Gorfinkiel J D and Tennyson J 2004 *J. Phys.B: At. Mol. Opt. Phys.* **37** L343–L350
[21] Gorfinkiel J D and Tennyson J 2005 *J. Phys.B: At. Mol. Opt. Phys.* **38** 1607–1622
[22] Munro J J, Walker B and Kang S Y 2011 Predicting plasma in wafer etch and deposition via quantum mechanics *Solid State Technology: Insight for Electronic Manufacturing*